INVESTIGATION OF THE COAL GASIFICATION PROCESS UNDER VARIOUS OPERATING CONDITIONS INSIDE A TWO-STAGE ENTRAINED FLOW GASIFIER

Armin Silaen and Ting Wang *
asilaen@uno.edu, twang@uno.edu
Energy Conversion & Conservation Center
University of New Orleans
New Orleans, Louisiana, USA

ABSTRACT

Numerical simulations of the coal gasification process inside a generic 2-stage entrained-flow gasifier fed with Indonesian coal at approximately 2000 metric tone/day are carried out. The 3-D Navier-Stokes equations and eight species transport equations are solved with three heterogeneous global reactions, three homogeneous reactions, and two-step thermal cracking equation of volatiles. The Chemical Percolation Devolatilization (CPD) model is used for the devolatilization process. Finite rates are used for the heterogeneous solid-to-gas reactions. Both finite rate and eddy-breakup combustion models are calculated for each homogeneous gas-to-gas reaction, and the smaller of the two rates is used. The water-shift reaction rate is adjusted to match available syngas composition from existing operational data without catalyst. This study is conducted to investigate the effects of different operation parameters on the gasification process including coal mixture (dry vs. slurry), oxidant (oxygen-blown vs. air-blown), and different coal distribution between two stages. In the two-stage coal-slurry feed operation, the dominant reactions are intense char combustion in the first stage and enhanced gasification reactions in the second stage. The gas temperature in the first stage for the dry-fed case is about 800 K higher than the slurry-fed case. This calls for attention of additional refractory maintenance in the dry-fed case. One-stage operation yields higher H_2, CO and CH_4 combined than if a two-stage operation is used, but with a lower syngas heating value. High heating value (HHV) of syngas for the one-stage operation is 7.68 MJ/kg, compared to 8.24 MJ/kg for two-stage operation with 72%-25% fuel distribution and 9.03 MJ/kg for two-stage operation with 50%-50% fuel distribution. Carbon conversion efficiency of the air-blown case is 77.3%, which is much lower than that of the oxygen-blown case (99.4%). The syngas heating value for the air-blown case is 4.40 MJ/kg, which is almost half of the heating value of the oxygen-blown case (8.24 MJ/kg).

1.0 INTRODUCTION

Gasification is the process of converting various carbon-based feedstocks to clean synthetic gas (syngas), which is primarily a mixture of hydrogen (H_2) and carbon-monoxide (CO) with minor methane (CH_4) and inert nitrogen gas, through an incomplete combustion. Feedstock is partially combusted with oxygen and steam at high temperature and pressure with only less than 30% of the required oxygen for complete combustion being provided. The syngas produced can be used as a fuel, usually for boilers or gas turbines to generate electricity, or can be used to make a synthetic natural gas, hydrogen gas or other chemical products. The gasification technology is applicable to any type of carbon-based feedstock, such as coal, heavy refinery residues, petroleum coke, biomass, and municipal wastes.

1.1 Global Gasification Chemical Reactions

This study only deals with global chemical reactions of coal gasification (Smoot and Smith, 1985) that can be generalized in reactions (R1.1) through (R1.9) below:

Heterogeneous (solid and gas) phase

$$C(s) + \tfrac{1}{2} O_2 \rightarrow CO, \quad \Delta H^\circ_R = -110.5 \text{ MJ/kmol} \qquad (R1.1)$$

$$C(s) + CO_2 \rightarrow 2CO, \quad \Delta H^\circ_R = +172.0 \text{ MJ/kmol} \qquad (R1.2)$$
(Gasification, Boudouard reaction)

$$C(s) + H_2O(g) \rightarrow CO + H_2, \quad \Delta H^\circ_R = +131.4 \text{ MJ/kmol} \qquad (R1.3)$$
(Gasification)

$$C + 2H_2 \rightarrow CH_4, \quad \Delta H^o_R = -87.4 \text{ MJ/kmol} \qquad (R1.4)$$
(Direct methanation)

Homogenous gas phase

$$CO + \tfrac{1}{2} O_2 \rightarrow CO_2, \quad \Delta H^\circ_R = -283.1 \text{ MJ/kmol} \qquad (R1.5)$$

$$CO + H_2O(g) \rightarrow CO_2 + H_2, \quad \Delta H^\circ_R = -41.0 \text{ MJ/kmol} \qquad (R1.6)$$
(Water-shift)

$$CO + 3H_2 \rightarrow CH_4 + H_2O, \quad \Delta H^o_R = -205.7 \text{ MJ/kmol} \qquad (R1.7)$$
(Methanation)

$$CH_{2.121}O_{0.5855} \rightarrow 0.5855CO + 0.2315H_2 + 0.4145CH_4 \qquad (R1.8)$$
(Volatiles cracking)

$$CH_4 + \tfrac{1}{2} O_2 \rightarrow CO + 2H_2 \qquad (R1.9)$$
(Volatiles gasification via CH_4)

In this study, the methanation reactions are not considered. Reactions (R1.8) and (R1.9) involve volatiles. The volatiles are modeled to go through a two-step thermal cracking (R1.8) and gasification processes (R1.9) via CH_4 as the intermediate product. The coal used in the study is sub-bituminous from Indonesia, whose compositions are given in Table 1a. It has a moisture content of 8.25%. Its moisture-free (MF) proximate and ultimate analyses compositions are listed in Table 1b. The compositions of volatiles are derived from the values of coal heating value, proximate analysis, and ultimate analysis.

Table 1a Compositions of Indonesian sub-bituminous coal.

	Weight %
Volatile	38.31%
H_2O	8.25%
ash	3.90%
C	37.95%
H	2.68%
N	0.69%
S	0.31%
O	7.91%
Total, wt %	100.00%
HHV, kcal/kg	5690

Table 1b Moisture-free (MF) compositions of Indonesian sub-bituminous coal.

Proximate Analysis (MF), wt%		***Ultimate Analysis (MF), wt%***	
Volatile	51.29	C	73.32
Fixed Carbon (FC)	47.54	H	4.56
Ash	1.17	O	20.12
	100.00	N	0.72
		S	0.11
		Ash	1.17
			100.00

1.2 Recent Research

Chen et al. (2000) developed a comprehensive three-dimensional simulation model for entrained coal gasifiers which applied an extend coal gas mixture fraction model with the Multi Solids Progress Variables (MSPV) method to simulate the gasification reaction and reactant mixing process. The model employed four mixture fractions and separately track the variable coal off-gas from the coal devolatilization, char-O_2, char-CO_2, and char-H_2O reactions. Chen et al. performed a series of numerical simulations for a 200 ton per day (tpd) two-stage air blown entrained flow gasifier developed for an IGCC process under various operation conditions (heterogeneous reaction rate, coal type, particle size, and air/coal partitioning to the two stages).

Bockelie et al. (2002) of Reaction Engineering International (REI) developed a CFD modeling capable of entrained flow gasifiers that focuses on two gasifier configurations: single-stage down fired system and two-stage with multiple feed inlets. The model was constructed using GLACIER, an REI in-house comprehensive coal combustion and gasification tool. The basic combustion flow field was established by employing full equilibrium chemistry. Gas properties were determined through local mixing calculations and are assumed to fluctuate randomly according to a statistical probability density function (PDF), which is characteristic of the turbulence. Gas-phase reactions were assumed to be limited by mixing rates for major species as opposed to chemical kinetic rates. Gaseous reactions were calculated assuming local instantaneous equilibrium. The particle reaction processes include coal devolatization, char oxidation, particle energy, particle liquid vaporization and gas-particle interchange. The model also includes a flowing slag sub-model.

The U.S. Department of Energy/National Energy Technology Laboratory (NETL) developed a 3D CFD model of two commercial-sized coal gasifiers [Guenther and Zitney (2005)]. The commercial FLUENT CFD software is used to model the first gasifier, which is a two-stage entrained-flow coal slurry-fed gasifier. The Eulerian-Lagrangian approach is applied. The second gasifier is a scaled-up design of transport gasifier. The NETL open source MFIX (Multiphase Flow Interphase eXchanges) Eulerian-Eulerian model is used for this dense multiphase transport gasifier. NETL also developed an Advanced Process Engineering Co-Simulator (APECS) that combines CFD models and plant-wide simulation. APECS enables NETL to couple its CFD models with steady-state process simulator Aspen Plus.

Silaen and Wang (2006) carried out a study that focused on the effect of flow injection directions on the gasification performance using the same generic two-stage entrained flow gasifier as studied by Chen et al. and Bockelie et al. Horizontal injection direction was compared to downward and upward direction. The results revealed that the horizontally tangential injection direction gave the best gasifier performance. Changing the direction of the first-stage injectors downward resulted in a carbon fuel conversion reduction, but produced more H_2. Changing the direction of the second-stage injectors, however, did little to affect the overall flow patterns due to the smaller-quantity of coal injection (25%); therefore the gasifier performance was essentially insignificantly affected.

Silaen and Wang (2010) conducted a study that investigates the effects of different parameters on gasification performance including five turbulence models, four devolatilization models and three coal particle sizes. The Eulerian-Lagrangian approach with finite global reaction rates was applied. A two-step decomposition model was applied to volatiles cracking and gasification via benzene as the intermediate product. The results revealed that the standard k-ε and the Reynolds Stress Model (RSM) models gave consistent results. Smaller particles have a higher surface/volume ratio, react faster than larger particles, and produce syngas with higher heating value than larger particles. High inertia possessed by larger coal particles propel the

particles cross the gas streamlines and increase particle-gas mixing which result in enhanced reaction rate, but they take longer to complete reaction of the entire particle. The single rate devolatilization model and the chemical percolation model produced moderate and consistent devolatilization rate.

This study is the continuous work of Silaen and Wang (2006, 2010) and focuses on investigating the effects of different operation parameters on the gasification process including coal mixture (dry vs. slurry), oxidant (oxygen-blown vs. air-blown), and different coal distribution between two stages.

2.0 COMPUTATIONAL MODEL

The computational model and submodels (devolatilization, reactions, particle dynamics, gasification) used in the study are the same as developed by Silaen and Wang (2010), so all equations and detailed modeling intricacies are not repeated here, but they are briefly summarized below. The time-averaged steady-state Navier-Stokes equations as well as the mass and energy conservation equations are solved. Species transport equations are solved for all gas species involved. The standard k-ε turbulence model is used to provide closure. Silaen and Wang (2010) applied five turbulence models (standard k-ε, k-ω, RSM, k-ω SST, and k-ε RNG) and reported that the standard k-ε turbulence model yields reasonable results without requiring very much computational time when compared to other turbulence models. Enhanced wall function and variable material property are used. The P1 model is used as the radiation model.

The flow (continuous phase) is solved in Eulerian form as a continuum while the particles (dispersed phase) are solved in Lagrangian form as a discrete phase. Stochastic tracking scheme is employed to model the effects of turbulence on the particles. The continuous phase and discrete phase are communicated through drag forces, lift forces, heat transfer, mass transfer, and species transfer. The finite-rate combustion model is used for the **heterogeneous** reactions, but both the finite-rate and eddy-dissipation models are used for the **homogeneous** reactions, and the smaller of the two is used as the reaction rate. The finite-rate model calculates the reaction rates based on the kinetics, while the eddy-dissipation model calculates based on the turbulent mixing rate of the flow. Gasification or combustion of coal particles undergoes the following global processes: (i) evaporation of moisture, (ii) devolatilization, (iii) gasification to CO and (iv) combustion of volatiles, CO, and char. The Chemical Percolation Devolatilization (CPD) model [Fletcher and Kerstein (1992), Fletcher et. al (1990), and Grant et. al (1989)] is chosen as the devolatilization model based on the finding by Silaen and Wang (2010) that the Kobayashi two-competing rates devolatilization model [Kobayashi et. al. (1976)] is very slow, while the CPD model gives a reasonable result.

For solid particles, the rate of depletion of the solid, due to a surface reaction, is expressed as a function of kinetic rate, solid species mass fraction on the surface, and particle surface area. The reaction rates are all **global net rates**, i.e., the backward reaction, calculated by equilibrium constants, are included in the global rate. Therefore, the finite rate employed in this study implicitly applies to the local equilibrium approach. Reaction rate constants used in this study are summarized in Table 2.

The reaction rate of the water-shift, adopted from Jones and Lindstedt (1988), is found to be too fast in this study because the rate is obtained with the presence of catalyst. Considering no catalyst is added in a typical gasifier, the water shift reaction rate is purposely slowed down to make the syngas composition consistent with that in the actual production of a commercial entrained-flow gasifier with coal-slurry feed from bottom.

For liquid droplets, water evaporates from the particle's surface when the temperature is higher than the saturation temperature (based on local water vapor concentration). The evaporation is controlled by the water vapor partial pressure until 100% relative humidity is achieved. When the boiling temperature (determined by the air-water mixture pressure) is reached, water continues to evaporate even though the relative humidity reaches 100%. After the moisture is evaporated, due to either high temperature or low moisture partial pressure, the vapor diffuses into the main flow and is transported away. Please refer to Silaen and Wang (2010) for details.

Table 2 Summary of reaction rate constants used in this study

Reaction	*Rate Constant*	*Parameters*
Solid-gas heterogeneous reactions:		
$C(s) + ½O_2 \rightarrow CO$ (Combustion)	$k = AT^n \exp(-E/RT)$	n = 0 A = 0.052 kg/m^2.Pa$^{-0.5}$ E = 6.1x10^7 J/kmol
$C(s) + CO_2 \rightarrow 2CO$ (Gasification, Boudouard reaction)	$k = AT^n \exp(-E/RT)$	n = 0 A = 0.0732 kg/m^2.Pa$^{-0.5}$ E = 1.125x10^8 J/kmol
$C(s) + H_2O(g) \rightarrow CO + H_2$ (Gasification)	$k = AT^n \exp(-E/RT)$	n = 0 A = 0.0782 kg/m^2.Pa$^{-0.5}$ E = 1.15x10^8 J/kmol
Gas phase homogeneous reactions:		
$CO + ½ O_2 \rightarrow CO_2$	$k = AT^n \exp(-E/RT)$	n = 0 A = 2.2x10^{12} E = 1.67x10^8 J/kmol
$CO + H_2O(g) \rightarrow CO_2 + H_2$ (Watershift)	$k = AT^n \exp(-E/RT)$	n = 0 A = 2.75x10^2 E = 8.38x10^7 J/kmol
$CH_{2.121}O_{0.5855} \rightarrow 0.5855CO + 0.2315H_2 + 0.4145CH_4$		Eddy-dissipation only
$CH_4 + ½O_2 \rightarrow CO + 2H_2$	Eddy-dissipation only	

The computation is carried out using the finite-volume-based commercial CFD software FLUENT 12.0 from ANSYS, Inc. The simulation is steady-state and uses the pressure-based solver, which employs an implicit pressure-correction scheme and decouples the momentum and energy equations. SIMPLE algorithm is used to couple the pressure and velocity. Second order upwind scheme is selected for spatial discretization of the convective terms. For the finite rate model where the Eulerian-Lagrangian approach is used, the iterations are conducted alternatively between the continuous

and the dispersed phases. Initially, two iterations in the continuous phase are conducted followed by one iteration in the discrete phase to avoid the flame from dying out. Once the flame is stably established, twenty iterations are performed in the continuous phase followed by one iteration in the dispersed phase. The drag, particle surface reaction, and mass transfer between the dispersed and the continuous phases are calculated. Based on the dispersed phase calculation results, the continuous phase is updated in the next iteration, and the process is repeated. Converged results are obtained when the residuals satisfy mass residual of 10^{-3}, energy residual of 10^{-5}, and momentum and turbulence kinetic energy residuals of 10^{-4}. These residuals are the summation of the imbalance in each cell, scaled by a representative for the flow rate. The computation was carried out in parallel processing on two dual-core Pentium clusters with 12 nodes each.

2.1 Physical Characteristics of the Model and Assumptions

This paper studies a two-stage entrained flow coal gasifier as shown in Fig. 1. Meshed computational domain is shown in Fig. 2. The grid consists of 1,106,588 unstructured tetrahedral cells. In the simulations, the buoyancy force is considered, varying fluid properties are calculated for each species and the gas mixture, and the walls are assumed impermeable and adiabatic. The flow is steady and no-slip condition (zero velocity) is imposed on the wall surfaces.

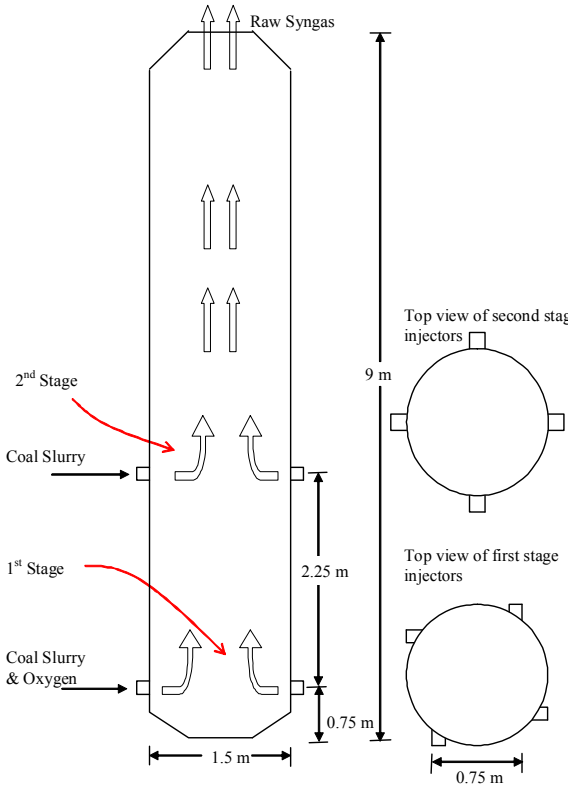

Fig. 1 Schematic of the two-stage entrained-flow gasifier.

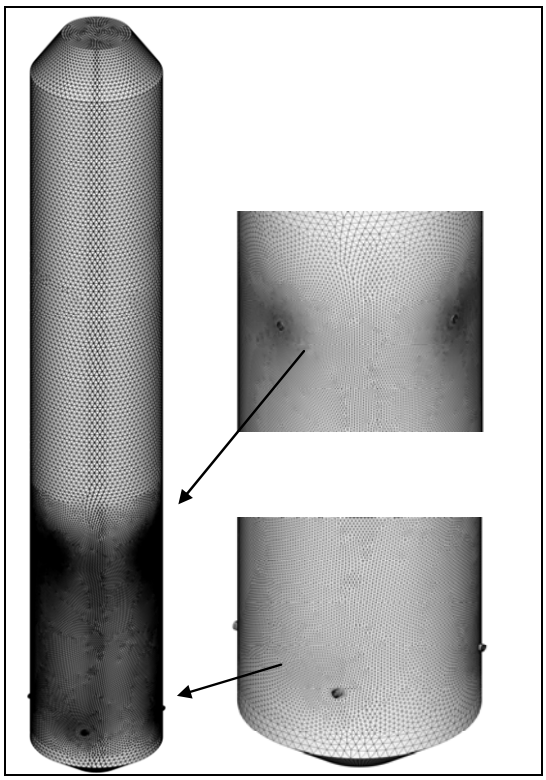

Fig. 2 Meshed computational domain of the two-stage entrained-flow gasifier.

3.0 BOUNDARY AND INLET CONDITIONS

Indonesian sub-bituminous coal is used as feedstock in this study; its composition is given in Table 1. Boundary conditions for the baseline case are shown in Fig. 3. The summary of the studied cases are listed in Table 3. In the baseline (Case 1) of this study, coal-slurry-fed and two-stage configuration is used with fuel distribution of 75%-25% between the first and the second stages. Total mass flow rates of the coal slurry and the oxidant are 21.9 kg/s and 9.92 kg/s, respectively. The total mass flow rate of the dry coal powder case (Case 2) is 12.90 kg/s. The difference in fuel mass flow rates is caused by water added for slurry. The moisture in the coal is included in both slurry and dry feed cases. The coal/water weight ratio of the coal slurry is 60%-40%. Oxidant/coal slurry feed rate gives O_2/coal equivalence ratio of 0.4. The equivalence ratio is defined as the percentage of oxidant provided over the stoichiometric amount for complete combustion.

The oxidant is considered as a continuous flow and coal slurry is considered as a discrete flow. The discrete phase only includes the fixed carbon and water from the moisture content of coal (8.25% wt) and water added to make the slurry. The slurry coal is treated as particles containing both coal and liquid water. Other components of the coal, such as N, H, S, O, and ash, are injected as gas, together with the oxidant in the continuous flow. N is treated as N_2, H as H_2, and O as O_2. S and ash are not modeled and their masses are lumped into N_2. The coal slurry size is uniformly given as 50

μm for the purpose of conveniently tracking the particle size reducing rate. Investigation of effects of coal particle size on gasification performance has been performed by Silaen and Wang (2009 and 2010) and is not repeated here.

The walls are assigned as adiabatic with internal emissivity of 0.8. The boundary condition of the discrete phase at walls is assigned as "reflect", which means the discrete phase elastically rebound off once reaching the wall. At the outlet, the discrete phase simply escapes/exits the computational domain. The gasifier is operating at 24 atm.

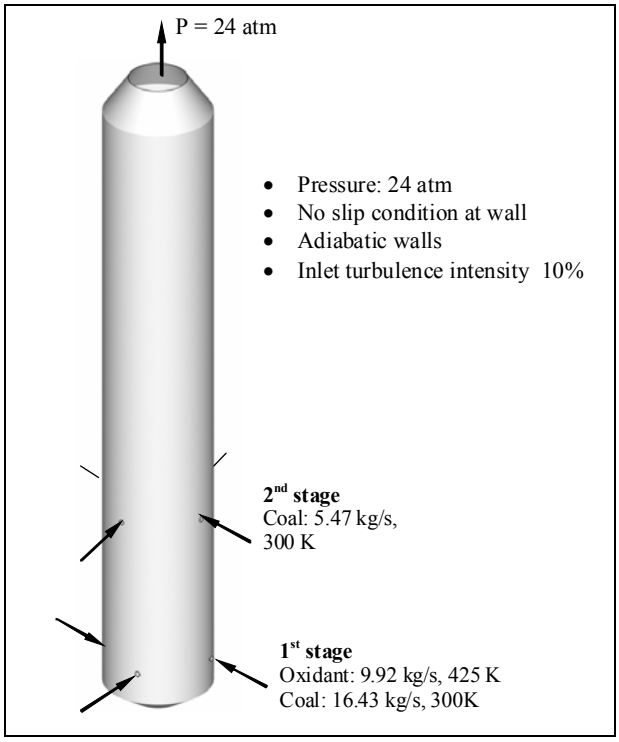

Fig. 3 Boundary conditions of the baseline case of the two-stage entrained-flow gasifier.

4.0 RESULTS AND DISCUSSIONS

The following five cases are studied:

Case 1: Baseline case, oxygen-blown, coal slurry, 75%-25% distribution in 2 stages
Case 2: Oxygen-blown, dry coal, 75%-25% distribution in 2 stages.
Case 3: Oxygen-blown, coal slurry, 50%-50% distribution in 2 stages.
Case 4: Oxygen-blown, coal slurry, 100% distribution in the 1st stage.
Case 5: Air-blown, coal slurry, 75%-25% distribution in 2 stages

4.1 Baseline Case (Case 1)

The baseline case (Case 1) is the two-stage oxygen-blown operation with coal slurry distribution of 75%-25% between the first and the second stages. Gas temperature and species mole fraction distributions on the horizontal and center vertical planes in the gasifier are shown in Fig. 4. The gas temperature is seen higher in the region between the first stage and second stage injection locations than in the region above the second stage injection location. Maximum gas temperature in the first stage reaches 2400K (3860°F). The dominant reaction in the first stage is the intense char combustion ($C + ½ O_2 \rightarrow CO$ and $CO + ½ O_2 \rightarrow CO_2$) in the first stage and gasification reactions (mainly char-CO_2 gasification, $C + ½ CO_2 \rightarrow CO$) in the second stage. Oxygen is completely depleted through the char combustion in the first stage. Char gasification is enhanced in the second stage with the injection of the remaining coal without oxygen. Char is gasified with CO_2 produced in the first stage through reaction $C + CO_2 \rightarrow CO$ and with H_2O through reaction $C + H_2O \rightarrow CO + H_2$.

Table 3 Parameter and operating conditions of the studied cases. The changed parameters are highlighted.

Parameters	*Case 1*			*Case 2*			*Case 3*			*Case 4*			*Case 5*		
Type															
Fuel	Slurry			**Dry**			Slurry			Slurry			Slurry		
Oxidant	Oxygen			Oxygen			Oxygen			Oxygen			**Air**		
Stage	*1*	*2*	*Total*	*1*	*2*	*Total*	*1*	*2*	*Total*	*1*	*2*	*Total*	*1*	*2*	*Total*
Distribution															
Fuel	75%	25%		75%	25%		**50%**	**50%**		**100%**	**0%**		75%	25%	
Oxidant	100%	0%		100%	0%		100%	0%		100%	0%		100%	0%	
Mass flow rate															
Fuel (kg/s)	16.43	5.47	21.9	9.47	3.16	12.90	10.95	10.95	21.90	21.90	0.00	21.90	8.12	2.70	10.82
Oxidant (kg/s)	9.92	0.00	9.92	9.92	0.00	9.92	9.92	0.00	9.92	9.92	0.00	9.92	21.00	0.00	21.00

*** Oxidant for Case 5 is air (78% N_2, 22% O_2).**

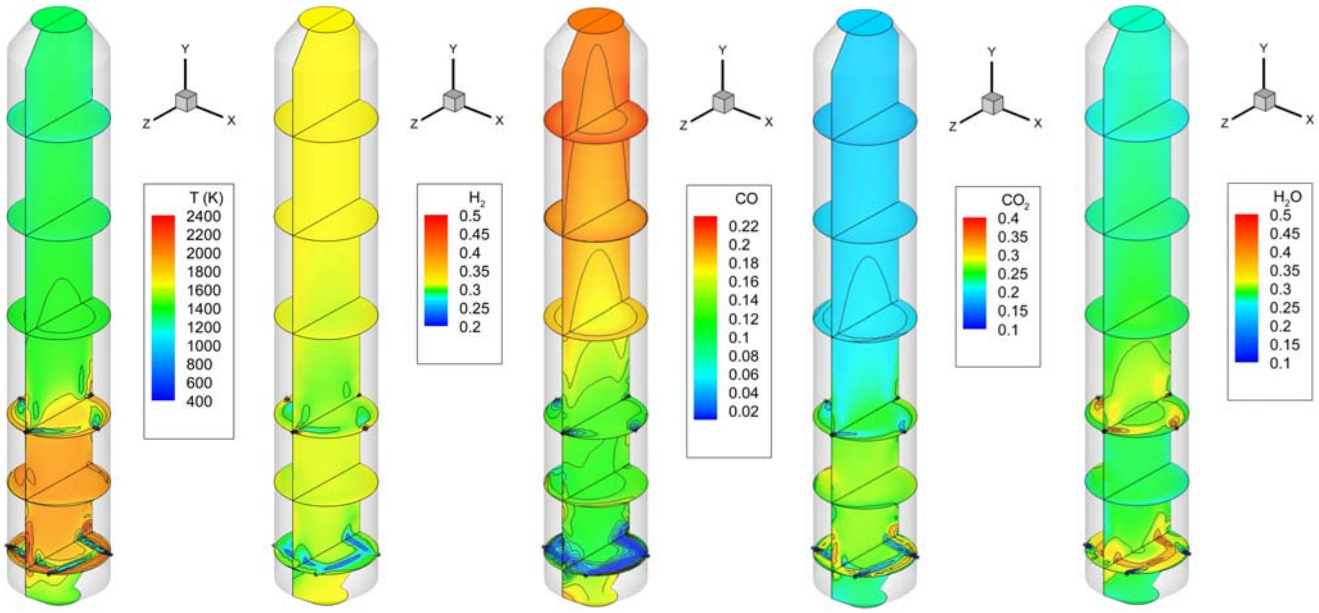

Fig. 4 Gas temperature and species mole fraction distributions for Case 1 (2-stage, 75%-25%, coal slurry, oxygen-blown).

Mass-weighted averages of gas temperature and species mole fractions along the gasifier height for Case 1 are shown in Fig. 5. The dips in the graphs occur at the injector elevations at heights of 0.75 m for the first stage and 3 m for the second stage. The CO_2 mole fraction and the gas temperature decrease from roughly 27% to roughly 19% as the gas flows from the first stage to the second stage. On the other hand, CO mole fraction increases from 12% to 20%, due to the endothermic char-CO_2 (R1.2) gasification mentioned above. Meanwhile, the increase in the average mole fraction of H_2 in the second stage is negligible. This may indicate that char-CO_2 gasification is more dominant than char-H_2O gasification in the second stage.

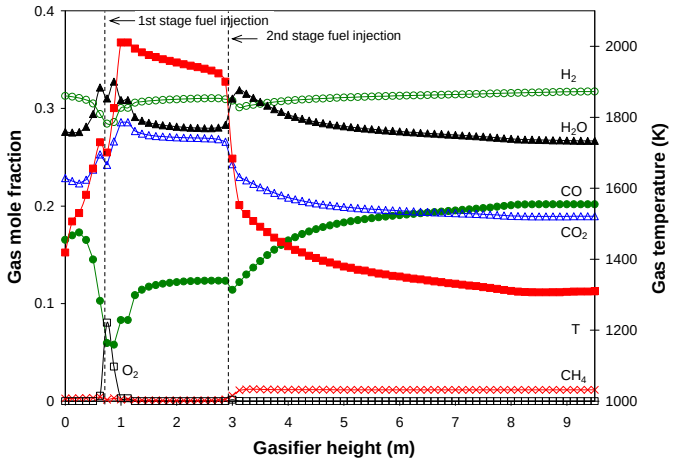

Fig. 5 Mass-weighted averages of gas temperature and species mole fraction distributions along gasifier height for Case 1 (2-stage, 75%-25%, coal slurry, oxygen-blown).

At the gasifier height of 8.5 m, the graphs for the average gas temperature and gas mole fractions flatten out. This indicates that the rates of reactions are slowing down. Making the gasifier longer or higher would probably not make significant change in the syngas temperature and compositions. The significant temperature drop from roughly 1900K (2960°F) to 1500K (2240°F) across the second stage clearly indicates the advantage of injecting only coal at the second stage to protect the refractory liner and reduce the maintenance cost.

Fig. 6a shows helical flow pathlines inside the gasifier; the helical pattern lengthens the flow residence time to allow more time for the reactions to take place. Velocity vectors on vertical midplane and horizontal injection levels are presented in Fig. 7. Due to the vortex generated by the tangential fuel injections in the first stage, strong upward flow occurs near the wall, and weak downward flow occurs in the center. The central core near the second stage exhibits an almost stagnant region due to the opposing fuel injections at the second stage. The flow below the first stage injection level is weak, which could result in some gas being trapped. The momentum of each jet in the second stage is not strong enough to reach the center, and hence the jets are swept upward by the strong main flow from the first stage. Figure 6b shows the coal particle distribution. The particles injected in the first stage are depleted fairly quickly, while those injected in the second stage are depleted at a slow rate.

Exit syngas temperature and mole fraction compositions are listed in Table 4. Carbon conversion efficiency is 99.4%, which is the comparison of the total mass of carbon injected into the gasifier to the total mass of carbon at the gasifier exit. The high heating value (HHV) of the exit syngas is 8.24 MJ/kg.

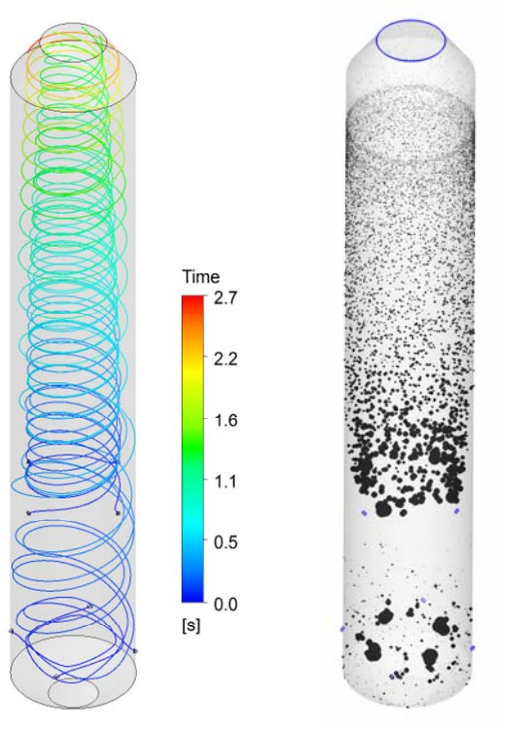

(a) (b)

Fig. 6 (a) Flow pathline colored by the residence time temperature and (b) particle distribution for Case 1.

Table 4 Exit syngas temperatures and compositions.

	Case 1	*Case 2*	*Case 3*	*Case 4*	*Case 5*
Fuel distribution	2-stage (75%-25%)	2-stage (75%-25%)	2-stage (50%-50%)	1-stage	2-stage (75%-25%)
Oxidant	oxygen	oxygen	oxygen	oxygen	air
Fuel type	slurry	dry	slurry	slurry	slurry
Exit syngas:					
T (K)	1310	1882	1250	1407	1143
T (°F)	1898	2928	1790	2073	1598
Mole fraction:					
H_2	31.7%	33.8%	31.1%	32.2%	19.0%
CO	20.2%	31.4%	19.7%	21.5%	7.6%
CO_2	18.9%	19.0%	19.2%	18.0%	12.5%
CH_4	1.2%	1.7%	1.3%	0.7%	0.4%
H_2O	26.7%	0.8%	27.4%	26.3%	16.4%
N_2	1.3%	13.3%	1.3%	1.3%	44.1%
O_2	0.0%	0.0%	0.0%	0.0%	0.0%
Carbon conversion efficiency	99.4%	100.0%	98.3%	94.8%	77.3%
HHV at 25°C (MJ/kg)	8.24	9.45	9.03	7.68	4.40

4.2 Effects of Coal Mixture (Slurry vs. Dry)

Case 2 is conducted to investigate the effects of using dry coal as the fuel. Coal and oxidant feed rates are kept the same as for Case 1. Nitrogen is used as the transport gas for the coal powder. The amount of N_2 transport gas used is 0.3 times the mass of coal powder. The same fuel and oxidant distributions as in Case 1 are used, which is two-stage operation with 75%-25% fuel distribution between the first and second stages and 100% oxidant injected into the first stage with no oxidant injection at the second stage.

The distribution of gas temperature presented in Fig. 8 shows that the local highest temperature in the first stage is approximately 3200 K (5300°F), which is 800 K (1440°F) higher than the coal slurry case (Case 1). Unlike the coal slurry case, the dry coal case does not have a lot of H_2O to absorb the heat released by the char combustion, nor does much water react with char through the char-H_2O gasification. H_2O presented in Case 2 comes from the moisture contained in the coal, while H_2O in Case 1 comes from both the moisture contained in the coal and water added to the coal to make the slurry. This higher gas temperature means that the fuel injectors and refractory liner in the first stage will experience more severe thermal loading and maintenance issues than in the coal slurry operation.

As seen in Fig. 9, the average CO mole fraction in the first stage is slightly higher than in the coal slurry case (Case 1), approximately 19% versus 12%. The same is observed for the average CO_2 and H_2 mole fractions, 30% for CO_2 and 34% for H_2 in the dry coal case compared to 27% for CO_2 and 31% for H_2 in the coal slurry case.

Similar to the coal slurry operation in Case 1, char gasification is enhanced in the second stage by injecting the remaining fresh coal. But because the coal injected is dry coal, char gasification that occurs is mainly char-CO_2 gasification.

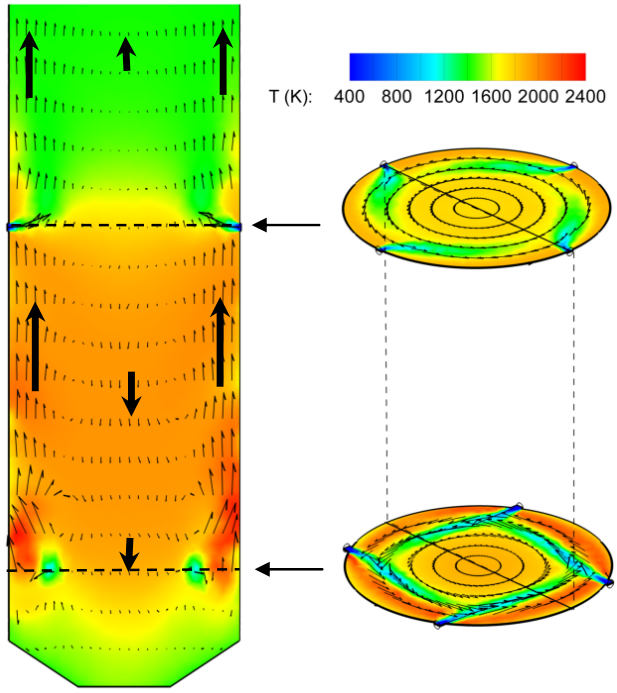

Fig. 7 Velocity vectors and temperature field on the center vertical plane and injection planes for Case 1.

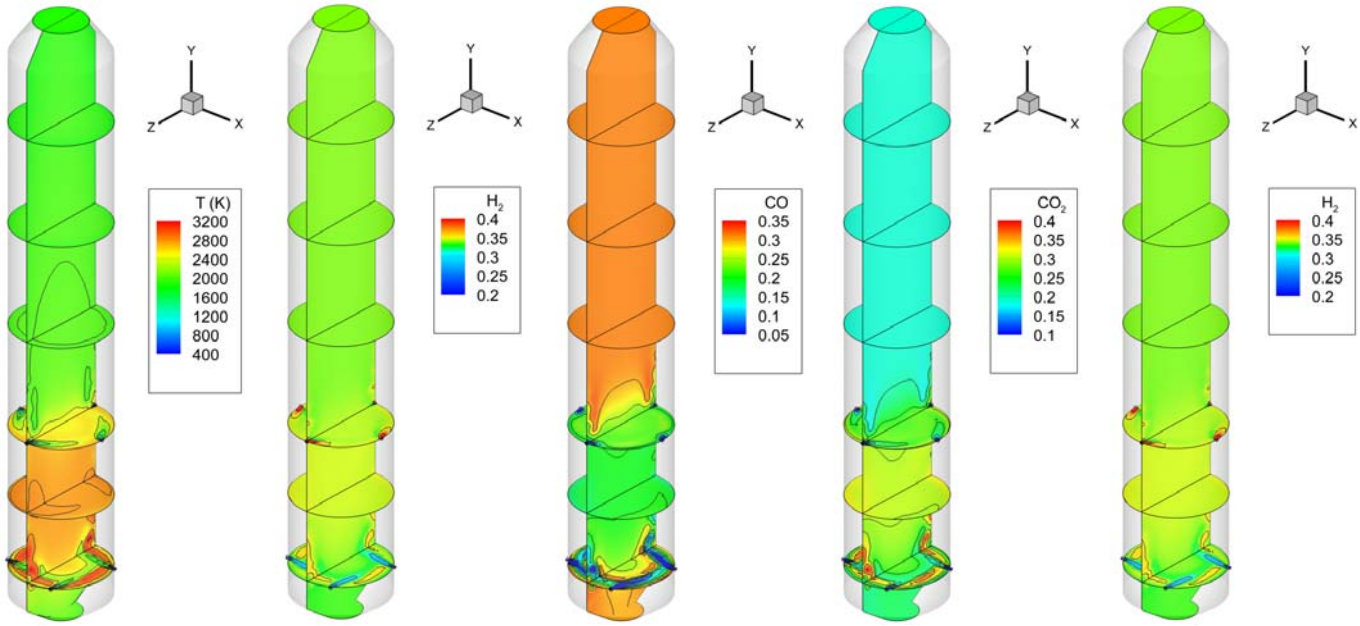

Fig. 8 Gas temperature and species mole fraction distributions for Case 2 (2-stage, 75%-25%, dry coal, oxygen-blown).

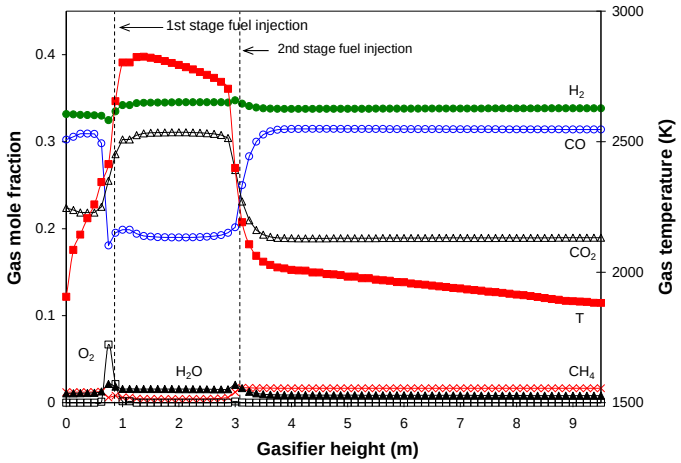

Fig. 9 Mass-weighted averages of gas temperature and species mole fraction distributions along gasifier height for Case 2 (2-stage, 75%-25%, dry coal, oxygen-blown).

Both Figs. 8 and 9 show a significant increase in CO (from approximately 19% to 31%) and decrease in CO_2 (from approximately 30% to 19%) in the second stage, due to the char-CO_2 gasification. Minor char-H_2O reaction also occurs in the second stage. The small decrease in H_2 in the second stage is due to dilution by the additional coal.

The average temperature of the exit syngas listed in Table 4 is 1882 K (2928°F), which is 572 K (1030°F) higher than the syngas for the coal slurry case (Case 1), due to lack of steam in the dry coal operation. Compared to the coal slurry case, there is less H_2O to absorb the heat from the char combustion and less H_2O to react with C through the endothermic char-H_2O reaction.

H_2 and CO_2 contents of the syngas are higher than those of the coal slurry case, 33.8% and 31.4% versus 31.7% and 20.2%, respectively. The syngas HHV of the dry coal case is also higher than the coal slurry case, 9.45 MJ/kg versus 8.24 MJ/kg. Of course, a higher heating value is better. However, in addition to potential increased maintenance issue related to fuel injectors and refractory liner, the higher syngas temperature of the dry coal case means that thermal efficiency will reduce when the syngas temperature is cooled down to the acceptable level for operating the downstream gas clean-up system. Although syngas cooler can transfer the thermal energy of the high raw syngas temperature to high-pressure steam, degradation of the energy quality will inevitably affect the overall plant thermal efficiency.

4.3 Effects of Fuel Distribution

In the baseline case (Case 1), fuel is distributed by 75%-25% between the first and the second stages. Cases 3 & 4 are conducted to study the effects of different fuel distributions. In Case 3, the fuel is evenly distributed between the first and the second stages, i.e. 50%-50%. In Case 4, all (100%) of the fuel is injected in the first stage. In other words, Case 4 simulates the one-stage operation of the gasifier. The same total feed rate of coal slurry and oxidant in Case 1 is used in Cases 3 & 4. As in Case 1, all of the oxidant is injected in the first stage.

Fig. 10 presents the comparison of average gas temperature and species mole fractions for Cases 1, 3, and 4. Higher mass-weighted average gas temperature 2500 K (4040°F) occurs in the first stage for Case 3 (50%-50%) compared to 1900 K (2960°F) of Case 1 (75%-25%) and is due to the higher O_2/char ratio in the first stage for Case 3. Higher O_2/char causes more char to burn, resulting in a higher average gas temperature. However, counter-intuitively, lower O_2/char ratio in Case 4 (100%-0%) in the 1st stage also produces higher average gas temperature than Case 1. A plausible explanation would be that the higher temperature in Case 3 is not actually caused by rich combustion as first thought, but it is caused by less water

presence, and hence, less heat capacity to absorb heat generated by combustion. This explanation can be supported by the high oxygen and CO_2 concentrations but low CO and H_2 concentration in the first stage of Case 3 shown in Fig. 10. This means combustion in the 1st stage in Case 3 is complete (i.e. high CO_2) but the gasification process is less productive (i.e. low CO and H_2). On the other hand, in Case 4 when 100% coal is injected in the 1st stage, oxygen is quickly consumed (i.e. low O_2) to produce CO with high temperature. The relatively lower average gas temperature in the injector area for Case 1 (75%-25%) has the benefit of helping prolong the life of fuel injectors and refractory liners.

The graph of O_2 mole fraction for Case 3 shows that a little amount of O_2 still exists when the gas reaches the second stage injection level. This means that char has a good opportunity to react with the abundant O_2 at the first stage. Meanwhile, for Case 1 (75%-25%) and Case 4 (100%-0%), O_2 is quickly completely depleted in the first stage. The comparison of CO and CO_2 mole fractions for all three cases confirms that char combustion is more intense in Case 3. Case 3 has the highest CO_2 mole fraction and the lowest CO mole fraction in the first stage. It implies that a large amount of char in the first stage goes through complete combustion. Case 4 (100%-0%), which has the lowest O_2/char ratio in the first stage, has the lowest CO_2 mole fraction and the highest CO mole fraction.

The exit syngas composition listed in Table 4 indicates that among the three cases, Case 4 (100%-0%) yields the highest H_2 production – 32.2% compared to 31.7% for Case 1 (75%-25%) and 31.1% for Case 3 (50%-50%). Case 4 also has the highest CO production – 21.5% compared to 20.2% for Case 1 and 19.7% for Case 3. However, Case 4 has the highest exit syngas temperature at 1407 K. Syngas temperature for Cases 1 and 3 are 1310 K and 1250 K, respectively.

Even though Case 4 has the highest H_2, CO and CH_4 combined, its syngas high heating value is the lowest among three cases. Case 4's HHV is 7.68 MJ/kg, compared to 8.24 MJ/kg for Case 1 and 9.03 MJ/kg for Case 3. This is due to the lower carbon conversion efficiency of Case 4 (94.8%) compared to the other two cases (99.4% for Case 1 and 98.3% for Case 3). The exit syngas of Case 4 contains the most unreacted char. Thus, combined with its high temperature, it has the lowest HHV. Note that when the syngas exit temperature is high more chemical energy has been converted to the sensible heat of the syngas and less chemical energy is reserved in the syngas. This sensible heat could be effectively used in the gas turbine combustor if the syngas could be fed directly into the gas turbine combustor without going through the gas cleanup. In reality, the sensible heat will be used to produce steam to produce power through the steam turbine because the syngas temperature needs to be reduced for cleaning and desulfurization.

Based on the syngas temperature and composition, the 50%-50% fuel distribution (Case 3) gives the best result. It has the highest syngas HHV (9.03 MJ/kg) even though its carbon conversion efficiency (98.3%) is slightly lower than that of the 75%-25% case (Case 1 with carbon conversion efficiency of 99.4%). Besides the highest syngas HHV, Case 3 has the lowest syngas temperature (1250 K, 1790°F). This lowest syngas temperature compared to the other cases means that there will be less energy loss during the syngas clean-up process. However, its mass-weighted average of gas temperature (2500 K, 4040°F) in the first stage is highest compared to those of the other cases, 1900 K (2960°F) for Case 1 and 1500 K (2240°F) for Case 4. This high gas temperature will put the gasifier's fuel injectors and wall refractory bricks in a higher thermal loading; consequently, they will be more prone to failure and require more maintenance.

Velocity vectors on vertical midplane and horizontal injection levels for Case 3 are presented in Fig. 10. With 50% of the fuel injected in the second stage, the fuel jests are stronger than in Case 1 (Fig. 7) and are able to penetrate deeper to the center crossing the upcoming flow from the first stage.

4.4 Effects of Oxidant (Oxygen-Blown vs. Air-Blown)

Case 5 simulates the air-blown two-stage operation of the gasifier. Air with composition of 22% O_2 and 78% N_2 by weight is used as the oxidant. The O_2/C mole ratio is maintained the same as in Case 1 (oxygen-blown) which is 0.4. Total feed rate of coal and oxidant combined is the same as for Case 1. Similar to Case 1, the fuel is distributed 75% and 25% between the first and the second stages.

As expected, the mass-weighted average of gas temperature in the first stage shown in Fig. 12 is lower than in Case 1 (oxygen-blown) due to the abundance of N_2 as a diluent in the air-blown case. The maximum cross-sectional mass weighted average gas temperature is approximately 1450 K (2150°F), while the maximum average gas temperature in the oxygen-blown case is 2000 K (3140°F).

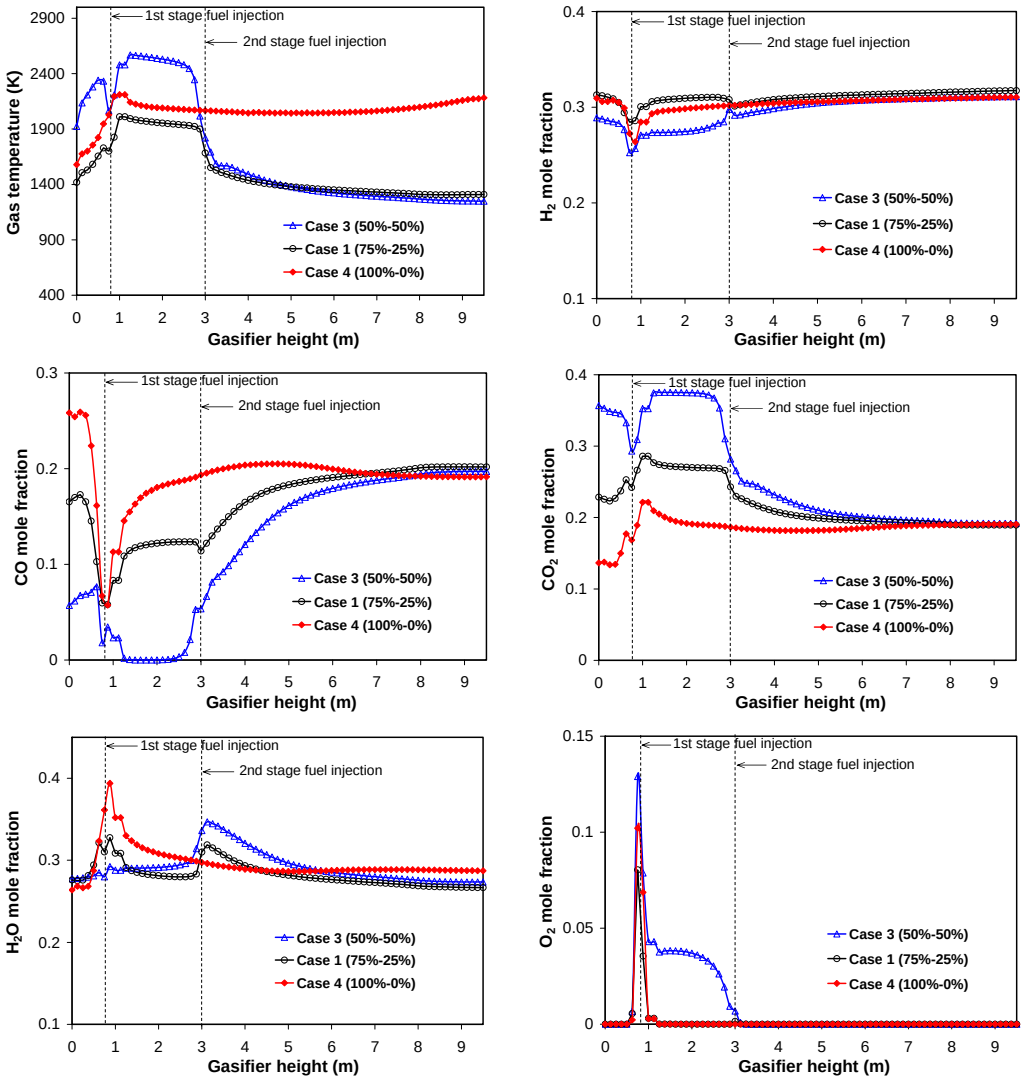

Fig. 10 Mass-weighted averages of gas temperature and species mole fraction distributions along gasifier height for Cases 1, 3 and 4.

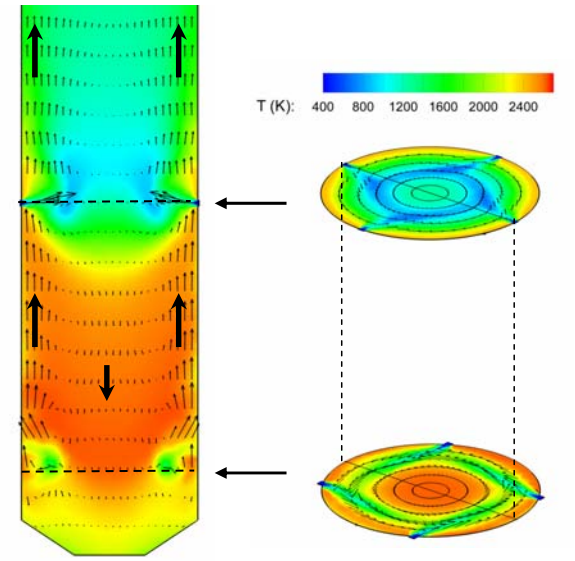

Fig. 11 Velocity vectors and temperature field on the center vertical plane and injection planes for Case 3 (50%-50%).

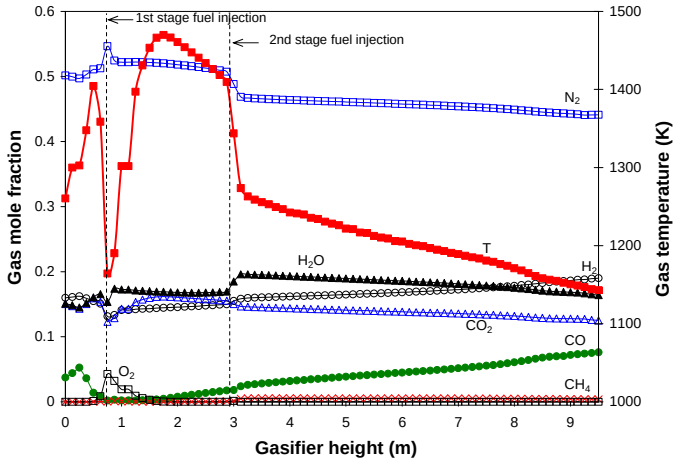

Fig. 12 Mass-weighted averages of gas temperature and species mole fraction distributions along gasifier height for Case 5 (2-stage, 75%-25%, coal slurry, air-blown).

Table 5 Comparison of exit syngas temperature and composition between Cases 1 and 5 after N_2 is removed from the syngas.

	Case 1	*Case 5*
Fuel distribution	2-stage (75%-25%)	2-stage (75%-25%)
Oxidant	oxygen	air
Fuel type	slurry	slurry
Exit syngas:		
T (K)	1310	1143
Mole fraction:		
H_2	32.1%	34.0%
CO	20.5%	13.6%
CO_2	19.1%	22.4%
CH_4	1.2%	0.7%
H_2O	27.1%	29.3%
O_2	0.0%	0.0%
Carbon conversion efficiency	99.4%	77.3%
HHV at 25°C (MJ/kg)	8.25	7.26

The syngas composition listed in Table 4 shows that the mole fraction ratio of CO/H_2 is 0.4 for the air-blown case (Case 5), which is much lower than those of the oxygen-blown case (Case 1). The syngas HHV for Case 5 is approximately only half of Case 1, 4.40 MJ/kg vs. 8.24 MJ/kg. The syngas of Case 5 is diluted with N_2, which causes this low heating value. However, its low carbon conversion efficiency at 77.3% also contributes to this low syngas heating value. Low carbon conversion efficiency is due to the lower overall gas temperature inside the gasifier, where less energy is available to drive the endothermic gasification reactions.

To give a fair comparison between the syngas in Cases 1 and 5, syngas compositions and heating values for both cases are recalculated after the N_2 contained in the syngas are removed. The recalculated compositions are compared in Table 5. The mole fraction of H_2 (34.0%) for the air-blown case (Case 5) becomes slightly higher than the oxygen-blown (Case 1, 32.1%), but the CO mole fraction for the air-blown (13.6%) is 6.5 percentage points lower than the oxygen-blown case. As expected, the heating value of the syngas increases from 4.40 MJ/kg to 7.26 MJ/kg after N_2 is removed. Nonetheless, this recalculated syngas heating value is still lower by roughly 1 MJ/kg than that of the oxygen-blown case (8.25 MJ/kg) even after N_2 is removed.

5.0 CONCLUSIONS

Five cases of different operating conditions are simulated and the results show:

Effects of Coal Mixture (Slurry vs. Dry)

The temperature in the first stage for the dry-fed case is approximately 2800 K (4580°F), which is 400 K (720°F) higher than the slurry-fed case. Unlike the slurry-fed case, the dry-fed case does not have a lot of H_2O to absorb the heat released by the char combustion, nor does much steam react with char through the char-H_2O gasification. This higher gas temperature means that the fuel injectors and refractory walls in the first stage will experience higher thermal loading than in the coal slurry operation. The syngas HHV of the dry coal case is also higher than the coal slurry case -- 9.45 MJ/kg vs. 8.24 MJ/kg. However, the higher syngas temperature of the dry coal case would result in a lower plant thermal efficiency because it needs to be cooled before it goes through the gas clean-up system downstream of the gasifier. Consequently, a lot of energy will be downgraded (i.e. loss of exergy) via waste heat exchanger even though part of the energy can be recovered to produce superheated steam to generate electricity through the steam turbine.

Effects of Fuel Distribution between Two Stages

Due to less water to absorb heat, reducing the fuel feed in the first stage does result in higher gas temperatures in the first stage. One-stage operation yields higher H_2, CO and CH_4 combined than if a two-stage operation is used but with a lower syngas heating value. The 50%-50% fuel distribution case yields the highest syngas HHV and lowest syngas exit temperature among the studied cases. The exit syngas of one-stage operation contains the most unreacted char, combined with its high exit temperature, results in the lowest heating value.

Effects of Oxidant (Oxygen-Blown vs. Air-Blown)

Gas temperature inside the gasifier for the air-blown case is lower than in the oxygen-blown gasifier due to the abundant presence of N_2. Lower than the oxygen-blown case (99.4%), the carbon conversion efficiency of the air-blown case is 77.3%. The syngas heating value for the air-blown case is 4.40 MJ/kg, which is almost half of the heating value of the oxygen-blown case (8.24 MJ/kg). Even when N_2 is removed for comparison, the HHV of the air-blown case is still about 1 MJ/kg less than the oxygen-blown case.

6.0 ACKNOWLEDGEMENTS

This study was supported by the Department of Energy contract No. DE-FC26-08NT01922 and the Louisiana Governor's Energy Initiative via the Clean Power and Energy Research Consortium (CPERC), administered by the Louisiana Board of Regents.

7.0 REFERENCES

Bockelie, M.J., Denison, K.K., Chen, Z., Linjewile, T., Senior, C.L., and Sarofim, A.F., CFD Modeling For Entrained Flow Gasifiers in Vision 21 Systems, Proceedings of the 19th Annual International Pittsburgh Coal Conference, Pittsburgh, PA. September 24-26, 2002.

Chen, C., Horio, M., and Kojima, T., Numerical Simulation of Entrained Flow Coal Gasifiers, Chemical Engineering Science, 55, 3861-3833, 2000.

Fletcher, T.H., and Kerstein, A.R., Pugmire, R.J., Grant, D.M., Chemical Percolation Model for Devolatilization: 2.

Temperature and Heating Rate Effects on Product Yields, Energy and Fuels, 4, 54, 1990.

Fletcher, T.H., and Kerstein, A.R., Chemical Percolation Model for Devolatilization: 3. Direct Use of ^{13}C NMR Date to Predict Effects of Coal Type, Energy and Fuels, 6, 414, 1992.

Grant, D.M., Pugmire, R.J., Fletcher, T.H., and Kerstein, A.R., Chemical Percolation of Coal Devolatilization Using Percolation Lattice Statistics, Energy and Fuels, 3, 175, 1989.

Guenther, C., and Zitney, S.E., Gasification CFD Modeling for Advanced Power Plant Simulation, Proceedings of the 22th International Pittsburgh Coal Conference, Pittsburgh, Pennsylvania, September 12-15, 2005.

Jones, W.P., and Lindstedt, R.P., Global Reaction Schemes for Hydrocarbon Combustion, Combustion and Flame,73,233,1998.

Kobayashi, H., Howard, J. B., and Sarofim, A. F., Coal Devolatilization at High Temperatures, 16th Symp. (Int'l.) on Combustion, The Combustion Institute, 1976.

Silaen, A. and Wang, T., Effects of Fuel Injection Angles on Performance of A Two-Stage Coal Gasifier, Proceedings of the 23rd Pittsburgh Coal Conference, Pittsburgh, Pennsylvania, Sept. 25-28, 2006.

Silaen, A. and Wang, T., Comparison of Instantaneous, Equilibrium and Finite Rate Gasification Models in an Entrained Flow Coal Gasifier, Paper 14-3, Proceedings of the 26th International Pittsburgh Coal Conference, Pittsburgh, Pennsylvania, Sept. 21-24, 2009.

Silaen, A. and Wang, T., Effect of Turbulence and Devolatilization Models on Gasification Simulation, International Journal of Heat and Mass Transfer, 53, 2074-2091, 2010.

Smoot, D.L., and Smith, P.J., Coal Combustion and Gasification, Plenum Press, 1985.